Thermal analysis of IGBT by isogeometric boundary element method

Yubo Guo
Materials and Manufacturing Department
Beijing University of Technology
Beijing, China
yuboGuo@emails.bjut.edu.cn

Huiping Yu
Materials and Manufacturing Department
Beijing University of Technology
Beijing, China
yuhuiping@emails.bjut.edu.cn

Yanpeng Gong
Materials and Manufacturing Department
Beijing University of Technology
Beijing, China
yanpeng.gong@bjut.edu.cn

Fei Qin
Materials and Manufacturing Department
Beijing University of Technology
Beijing, China
qfei@bjut.edu.cn

***Abstract*—IGBT as the core device of power conversion and control is widely applied in advanced manufacturing, national defense industry and other fields required electric energy. Studies show that inhomogeneous distribution of temperature caused by chip is a major factor resulted in failure of electronic devices. BEM is a commonly used method for the analysis of heat conduction problems. In recent years, IGABEM which provides some key advancements is a new development of BEM. Based on the IGABEM, a method for the heat conduction of IGBT devices is proposed. The reliability of the algorithm is examined by the consistency of numerical and analytical solutions.**

Keywords—*IGBT, Isogeometric boundary element, Thermal analysis*

I. INTRODUCTION

Insulated gate bipolar transistor (IGBT) is widely applied in many fields [1]. IGBT devices are generally composed of multilayered structure, including chip, direct bonding copper (DBC) substrate and so on [2]. Researches [3] show that temperature is responsible for about 60% of electronic product failures.

In the past decades, tremendous effort was devoted to derive experimental techniques or convenient numerical models for analyzing temperature distribution of IGBT. Fang and his collaborators [2] analyzed the thermal and mechanical performances of IGBT under the condition of power cycle by experiments means. Actually, due to the high cost, low efficiency and difficult data acquisition of experimental research, numerical analysis is becoming well received by researchers. In recent years, finite element method (FEM) is commonly applied in the simulation of IGBT devices. Compared with FEM, boundary element method (BEM) has many advantages, such as dimension reduction, high accuracy and easy to solve heat conduction and fracture problems [4]. In 2004, Khatir and his collaborators [5] proceeded the thermal fatigue of IGBT by BEM. The results show that BEM is a very promising approach to study high power IGBT module. In 2005, Hughes and his collaborators [6] put forward the isogeometric analysis (IGA) by straightway using data represented by NURBS basis functions. In recent years, the combination of isogeometric analysis and BEM (called IGABEM) is a new development of BEM. In 2019, Gong et al. [4] proposed a 2D IGABEM for thermal barrier coatings and confirmed its high computational efficiency in solving multilayer structure problems. Because of its advantages of high precision and boundary-only discretization, IGABEM gained rapid development and became a powerful tool in the analysis of models with complex geometries or thin structures (i.e. IGBT and other semiconductor devices with multilayer structures).

In this work, based on IGABEM the heat conduction problems of IGBT devices are studied. Domain integrals caused by heat source (chip) will be converted into boundary integrals using the radial integration method [7]. Thus a pure boundary integral equation (BIE) for heat conduction of IGBT is established. The subdomain BEM is used to study the heat transfer problems of DBC substrate which is composed of different materials. In the computation, the DBC substrate is divided into several regions. And independent linear system in different subdomains can be established. By solving the equations, unknown temperatures and fluxes of the corresponding nodes can be obtained.

II. METHOD

A. Implementation of IGABEM with heat source

The BIE of steady-state heat conduction problems in domain Ω (with boundary Γ) can be derived as follows [7]:

$$\begin{aligned} c(p)t(p) = &-\int_\Gamma u^*(Q,p)q(Q)d\Gamma(Q) \\ &-\int_\Gamma q^*(Q,p)\,t(Q)d\Gamma(Q) \\ &+\int_\Omega u^*(q,p)b(q)d\Omega(q) \end{aligned} \tag{1}$$

where u^* and q^* are the fundamental solutions, which can be defined as:

$$u^* = -\frac{1}{2\pi}\ln r \tag{2}$$

$$q^* = \frac{\partial u^*}{\partial \mathbf{n}} = \frac{\partial u^*}{\partial r}\frac{\partial r}{\partial \mathbf{n}} = -\frac{1}{2\pi r}\frac{\partial r}{\partial \mathbf{n}} \tag{3}$$

This research is supported by the Beijing Postdoctoral Research Foundation.

$r = r(Q,p) = \|Q - p\|$ represents the distance from source point to field point.

For any inner point p' ($\in \Omega$), its temperature can be obtained by the following formulation [7]:

$$\begin{aligned} t(p') = &-\int_\Gamma u^*(Q,p')q(Q)d\Gamma(Q) \\ &-\int_\Gamma q^*(Q,p')t(Q)d\Gamma(Q) \\ &+\int_\Omega u^*(q,p')b(q)d\Omega(q) \end{aligned} \tag{4}$$

The last terms in (1) and (4) are domain integrals, which is a challenging problem for BEM. As shown in (5), the radial integral method [7] is adopted to convert to boundary integrals:

$$\begin{aligned} &\int_\Omega u^*(q,p)b(q)d\Omega(q) \\ &= \int_\Gamma \frac{1}{r^\alpha(Q,p)}\frac{\partial \mathrm{r}}{\partial \mathbf{n}}F(Q,p)d\Gamma(Q) \end{aligned} \tag{5}$$

where

$$F(Q,p) = \int_0^{r(Q,p)} u^*(q,p)b(q)r^\alpha(q,p)dr(q) \tag{6}$$

By substituting (5) into (1), the BIE with boundary-only discretization is obtained as follows:

$$\begin{aligned} c(p)t(p) = &-\int_\Gamma u^*(Q,p)q(Q)d\Gamma(Q) \\ &-\int_\Gamma q^*(Q,p)t(Q)d\Gamma(Q) \\ &+\int_\Gamma \frac{1}{r^\alpha(Q,p)}\frac{\partial r}{\partial n}F(Q,p)d\Gamma(Q) \end{aligned} \tag{7}$$

By considering knot spans, the boundary Γ can be divided into isogeometric elements Γ_e (e=1,2,…,N). The boundary geometry $\mathbf{x} = (x_1, x_2, x_3)$, temperature t and flux density q can be expressed by a NURBS basis expansion, i.e.

$$\mathbf{x}(\xi) = \sum_{a=1}^{p+1} R_{a,p}(\xi)\mathrm{P}_a \tag{8}$$

$$t(\xi) = \sum_{a=1}^{p+1} R_{a,p}(\xi)t_a \tag{9}$$

$$q(\xi) = \sum_{a=1}^{p+1} R_{a,p}(\xi)q_a \tag{10}$$

where $R_{a,p}(\xi)$ is the ath local NURBS basis function of degree p [6]; P_a the control point of considered element Γ_e; t_a local temperature; q_a local flux.

Here a brief introduction about the implementation of IGABEM with heat source will be given. As shown in Fig. 1, the chip of IGBT is simplified as a quadrilateral structure. The parameter definition of the model is described by knot vector {0,0,0,1,1,2,2,3,3,4,4,4}. The boundary is described by p-order NURBS (p=2) and discretized into four isogeometric elements .

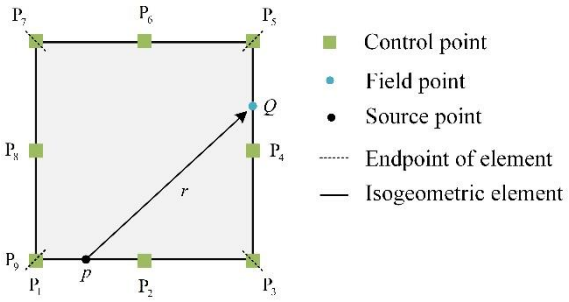

Fig. 1. Isogeometric model of the considered chip.

The discretized BIE can be obtained by using (9) and (10):

$$\begin{aligned} &c(\zeta_c)\sum_{l=1}^{p+1} N_l^e(\zeta_c)t^{le} = \\ &-\sum_{e=1}^{N_e}\sum_{l=1}^{p+1}\left[\int_{-1}^{1} u^*(\zeta_c,\hat{\xi}_e)N_l^e(\hat{\xi}_e)J(\hat{\xi}_e)d\hat{\xi}_e\right]q^{le} \\ &-\sum_{e=1}^{N_e}\sum_{l=1}^{p+1}\left[\int_{-1}^{1} q^*(\zeta_c,\hat{\xi}_e)N_l^e(\hat{\xi}_e)J(\hat{\xi}_e)d\hat{\xi}_e\right]t^{le} \\ &+\sum_{e=1}^{N_e}\left[\int_{-1}^{1}\frac{1}{r^\alpha(\zeta_c,\hat{\xi}_e)}\frac{\partial r}{\partial \mathbf{n}}F^e(\zeta_c,\hat{\xi}_e)J(\hat{\xi}_e)d\hat{\xi}_e\right] \end{aligned} \tag{11}$$

where e is the element index. N^e represents the element number. J is the Jacobian of coordinate transformation. $\zeta_c \in [0,1]$ and $\hat{\xi}_e \in [-1,1]$ are the local coordinate of source point and field point. t^{le} and q^{le} are the lth temperature and heat flow values in e, respectively. The values of J can be achieved by (12):

$$J(\hat{\xi}_e) = \frac{d\Gamma}{d\xi_e} = \frac{d\Gamma}{d\xi_e}\frac{d\xi_e}{d\hat{\xi}_e} \tag{12}$$

Through considering (11) at a certain number of collocation points, a system of equations can be assembled into a matrix form:

$$\mathbf{Ht}+\mathbf{Gq} = \boldsymbol{y_b} \tag{13}$$

where the matrices $\mathbf{H} = \left[H_{ij}\right]$ and $\mathbf{G} = \left[G_{ij}\right]$ contain the integrals of fundamental solutions u^* and q^*, i.e.

$$H_l^{ij} = \int_{-1}^{1} q^*(\zeta_c,\hat{\xi}_e)N_l^e(\hat{\xi}_e)J(\hat{\xi}_e)d\hat{\xi}_e \tag{14}$$

$$G_l^{ij} = \int_{-1}^{1} u^*(\zeta_c,\hat{\xi}_e)N_l^e(\hat{\xi}_e)J(\hat{\xi}_e)d\hat{\xi}_e \tag{15}$$

$\boldsymbol{y_b}$ is a column matrix.

By using boundary conditions, equation (13) can be reassembled to form the following linear system:

$$\boldsymbol{A\lambda} = \boldsymbol{b} \tag{16}$$

where matrix $\boldsymbol{A}$ contains values of integrals related to the unknown temperatures and fluxes. $\boldsymbol{\lambda}$ includes the unknown temperatures and fluxes coefficients. And $\boldsymbol{b}$ is the column vector with known data. All the temperatures and fluxes on the boundary can be obtained by solving (16) using any solver capable of dealing with a dense nonsymmetric matrix.

Then the temperatures inside the model can be obtained by using (4).

B. *Implementation of multi-domain IGABEM on DBC substrate*

To realize the thermal analysis of IGBT module, the multi-domain IGABEM will be used. The basic idea of multi-domain IGABEM is to divide the whole computed model into several subregions according to material/geometry properties, and then establish independent linear system for each sub domain.

Here we will apply the multi-domain IGABEM to study the temperature distribution on the DBC substrate in IGBT devices. As demonstrated in Fig. 2, DBC substrate is composed of three kinds of materials, including the upper/bottom copper layer and ceramic layer. According to the regular BEM, the BIE in each region can be expressed as [4]

$$c(p)t(p)+\int_{\Gamma_I} q^*(Q,p)t(Q)d\Gamma(Q)=\int_{\Gamma_I} u^*(Q,p)q(Q)d\Gamma(Q) \quad (17)$$

where Γ_I $(I = 1, 2, 3)$ represents the boundary of subdomain Ω_I.

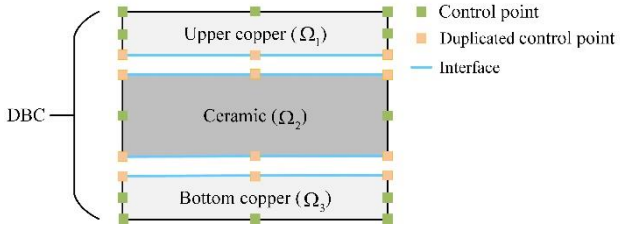

Fig. 2. DBC substrate model. ($\Omega=\Omega_1+\Omega_2+\Omega_3$)

To solve the problem, the following relationships resulted from physical considerations (called continued conditions) at the interfaces will be adopted.

$$\left.\begin{aligned}\mathbf{t}^1&=\mathbf{t}^2\\ \mathbf{q}^1&=-\mathbf{q}^2\end{aligned}\right\}\ \text{along the interface between } \Omega_1 \text{ and } \Omega_2$$
$$\left.\begin{aligned}\mathbf{t}^3&=\mathbf{t}^2\\ \mathbf{q}^3&=-\mathbf{q}^2\end{aligned}\right\}\ \text{along the interface between } \Omega_2 \text{ and } \Omega_3 \quad (18)$$

Substituting the temperature and flux in (9) and (10), the discretized form of BIE in (17) can be achieved:

$$\begin{aligned}&c(\zeta_c)\sum_{l=1}^{p+1}N_l^e(\zeta_c)t^{le}\\ &+\sum_{e=1}^{N_e}\sum_{l=1}^{p+1}\left[\int_{-1}^{1}q^*(\zeta_c,\hat{\xi}_e)N_l^e(\hat{\xi}_e)J(\hat{\xi}_e)d\hat{\xi}_e\right]t^{le}\\ &=\sum_{e=1}^{N_e}\sum_{l=1}^{p+1}\left[\int_{-1}^{1}u^*(\zeta_c,\hat{\xi}_e)N_l^e(\hat{\xi}_e)J(\hat{\xi}_e)d\hat{\xi}_e\right]q^{le}\end{aligned} \quad (19)$$

Considering the discretized boundary equations of three domains, one can obtain the following systems:

$$\begin{aligned}\mathbf{H}^1\mathbf{t}^1&=\mathbf{G}^1\mathbf{q}^1\\ \mathbf{H}^2\mathbf{t}^2&=\mathbf{G}^2\mathbf{q}^2\\ \mathbf{H}^3\mathbf{t}^3&=\mathbf{G}^3\mathbf{q}^3\end{aligned} \quad (20)$$

where matrices **H** and **G** contain integrals indicated in (14) and (15). Application of the boundary conditions and continuity conditions in (19), then the following linear system can be obtained.

$$\boldsymbol{A}\boldsymbol{\lambda}=\boldsymbol{b} \quad (21)$$

Here, matrix $\boldsymbol{A}$ contains values of integrals related to unknown temperatures and fluxes in three domains. $\boldsymbol{\lambda}$ includes unknown temperature and flux coefficients. $\boldsymbol{b}$ is the column vector consisted of known values.

After all temperatures and fluxes are obtained, the temperature at any point $p' \in \Omega$ can be computed by the following formulation:

$$t(p')=\int_{\Gamma_I} u^*(Q,p')q(Q)d\Gamma(Q)-\int_{\Gamma_I} q^*(Q,p')t(Q)d\Gamma(Q) \quad (22)$$

III. RESULTS AND DISCUSSION

A. *Temperature distribution of a chip model*

In order to check the correctness of the present isogeometric boundary element algorithm, consider a chip with square plate structure as shown in Fig. 1. In this model, temperatures on left and right sides are prescribed as 100°C. Upper and lower boundaries are insulation. Assume the thermal conductivity of computed model is 1 W/(m·K). And the heat source in the domain is $b(x)=1000\,\mathrm{W/m^3}$. The exact solution for temperature in the model can be computed by:

$$\mathrm{t}=-500\mathrm{x}^2+500\mathrm{x}+100 \quad (23)$$

To carry out the accuracy of presented method, relative errors (Re) are defined as

$$\mathrm{Re}=\frac{\left|t_{\mathrm{num}}-t_{\mathrm{exact}}\right|}{\left|t_{\mathrm{exact}}\right|} \quad (24)$$

In Fig. 3, the Re achieved by the proposed IGABEM are presented, which shows the algorithm can get very accurate results (Re < 4‰) by using only four isogeometric elements. And Fig. 3 also implies the put forward IGABEM can obtain satisfactory results for chip model with heat source.

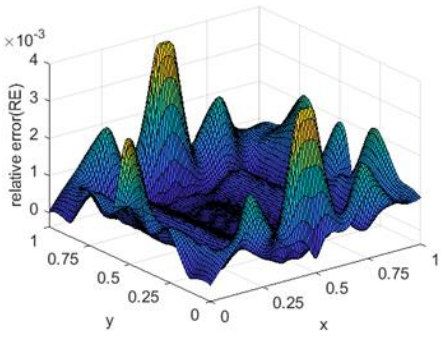

Fig. 3. RE of the computed points.

To further study the effectiveness of the proposed IGABEM. A chip model with internal heat source being a quadratic function $b(\mathrm{x})=600(\mathrm{x}^2+\mathrm{xy})$ will be considered. Heat fluxes of upper and lower boundaries are given as 5 W/m, and temperatures on left and right boundaries are 45°C. Fig. 4 displays the temperature field of chip for the current boundary condition. It shows that even if the heat source is a

quadratic function, internal temperatures can be effectively obtained by using the proposed algorithm. From Fig. 4 we can see that the highest temperature appears in the area close to the top boundary. A FEM model with 100 elements and 121 nodes is established by the Abaqus to offer a reference solution. The temperatures computed by Abaqus is demonstrated in Fig. 5, which illustrates that the results obtained by FEM and IGABEM (given in Fig. 4) have same change tendency.

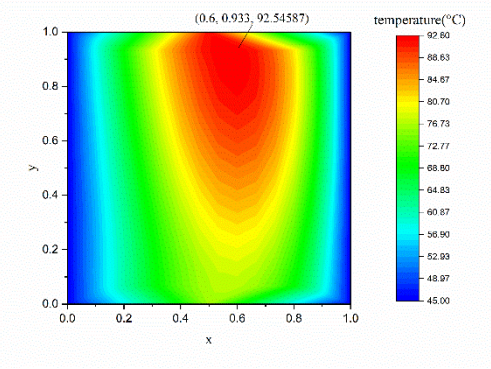

Fig. 4. The highest temperature (92.54587°C) presents to the point (0.6, 0.933).

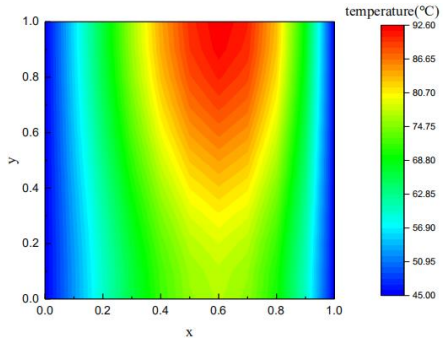

Fig. 5. Temperature field achieved by ABAQUS.

B. Temperature distribution of DBC substrate

As demonstrated in Fig. 6, a classical DBC substrate of IGBT will be studied. The middle layer ceramic plate (with thermal conductivity coefficients $\lambda = 20$ W/(m·K)) is a 1×0.3 mm^2 plate. Top and bottom are consisted of copper structures with $\lambda = 400$ W/(m·K). The initial thickness of upper copper and bottom copper is 0.4 mm. Fig. 6 shows the boundary condition setting of DBC substrate. The laterality are insulation, i.e. $\partial t/\partial \mathbf{n} = 0$. The temperatures on top and bottom boundaries are described as T_1 = 10°C and T_2 = 90°C.

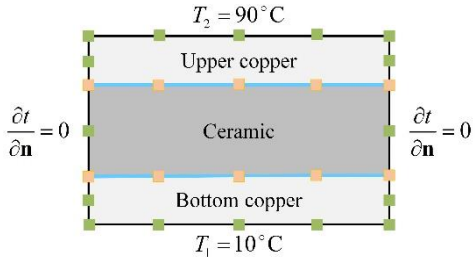

Fig. 6. Boundary condition of DBC substrate.

Here, the model is discretized into only 14 isogeometric elements. Fig. 7 gives the temperature field of the DBC model. It can be seen that since the characteristics of high thermal conductivity and low thermal resistance, the temperature loss in upper and bottom copper layers is smaller than that in the middle ceramic layer. In addition, due to differences of material properties, the temperature change near interfaces can be seen clearly.

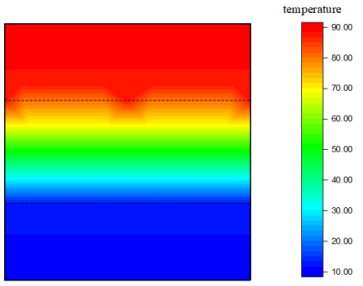

Fig. 7. Temperature field distribution of DBC substrate.

Temperatures are computed at points inside the boundary with parameter coordinates (0.5, y). Fig. 8 shows that the present results and exact solutions are consistent. Furthermore, it takes 59 seconds to calculate the temperatures at 1,283 internal points, which means that the present algorithm is efficient and time-saving.

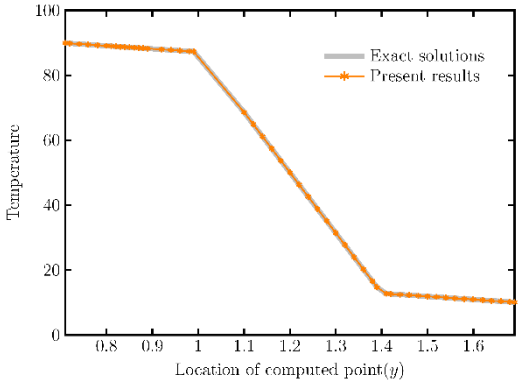

Fig. 8. The change of temperature tracing the line (0.5, y).

In Fig. 9, we study the effect of each layer thickness on the heat transfer. In the computation, the thickness of ceramic layer remains fixed at 0.4 mm and the copper plate thickness varies from 0.2 to 0.35 mm. Since the material discontinuity of the model, all the temperature curves are divided into three parts. Table I shows temperature values at the computed points that are located at the interface. Although the temperature curves have similar tendency for different thickness, as copper layer's thickness increases, the gradient of the curve increasingly decelerates.

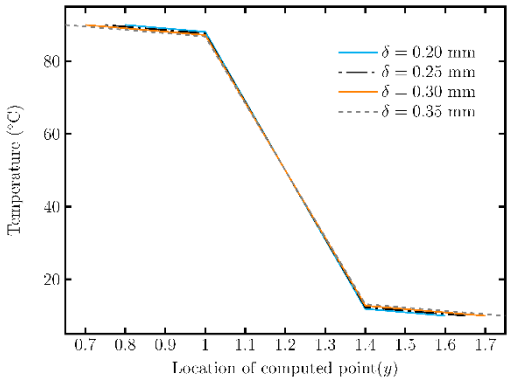

Fig. 9. Temperatures along the curve (0.5, y) for copper layer with different thickness δ .

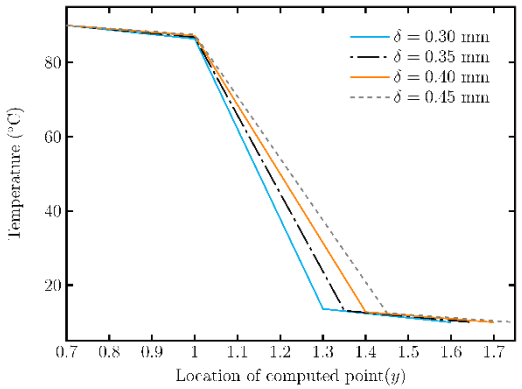

Fig. 10. Temperatures along the curve (0.5, y) for ceramic layer with different thickness δ .

TABLE I. INTERFACE TEMPERATURES (°C) WITH THE CHANGE OF COPPER LAYER THICKNESS (δ)

δ (mm)	**0.2**	**0.25**	**0.3**	**0.35**
Interface1	88.09438	87.64647	87.20892	86.78143
Interface2	11.90562	12.35352	12.79107	13.21856

TABLE II. INTERFACE TEMPERATURES (°C) WITH THE CHANGE OF CERAMIC LAYER THICKNESS (δ)

δ (mm)	**0.3**	**0.35**	**0.4**	**0.45**
Interface1	86.36363	86.84185	87.20892	87.49954
Interface2	13.63636	13.15814	12.79107	12.50045

To further study relationships between the thickness of ceramic layer and temperatures, the thickness of the upper and bottom copper layers remains fixed at 0.3 mm and ceramic layer thickness vary from 0.3 to 0.45 mm. The temperature curve for different cases is given in Fig. 10, and the Table II lists the temperature values at interfaces. From Fig. 10 we can see that along computed points the temperature curve is still divided into three parts. With the increase of ceramic layer thickness, the slopes of temperature curve slow down, but the temperatures difference increase. Actually, the increase of temperature difference might bring a certain risk of failure. Therefore, it is beneficial for the structure to reduce the thickness of the ceramic layer under a certain thickness of copper layer.

IV. CONCLUSION

A 2D IGABEM with heat source is developed and the temperature distribution of chip and DBC substrate for IGBT module are analyzed by using the present method.

ACKNOWLEDGMENT

This research is supported by the Beijing Postdoctoral Research Foundation.

REFERENCES

[1] C. Durand, M. Klingler, D. Coutellier and H. Naceur, “Power cycling reliability of power module: A survey,” IEEE T. Device Mat. Re., vol. 16, pp. 80-97, Jan. 2016.

[2] C. Fang, T. An, F. Qin, J. Zhao and X. Yuan, “Temperature and stress distribution of IGBT module in DC power cycling test with different switching frequencies,” ICEPT, China, pp. 785-790, Aug. 2018.

[3] P. M. Fabis, D. Shum and H. Windischmann, “Thermal modeling of diamond-based power electronics packaging,” IEEE, pp. 98-104, Mar. 1999.

[4] Y. Gong, J. Trevelyan, G. Hattori and C. Dong, “Hybrid nearly singular integration for isogeometric boundary element analysis of coatings and other thin 2D structures,” Comput. Method. Appl. M., vol. 346, pp. 642-673, Dec. 2019.

[5] Z. Khatir and S. Lefebvre, “Boundary element analysis of thermal fatigue effects on high power IGBT modules,” Microelectron. Reliab., vol. 44, pp. 929-938, Jun. 2004.

[6] T. J. R. Hughes, J. A. Cottrell and Y. Bazilevs, “Isogeometric analysis: CAD, finite elements, NURBS, exact geometry and mesh refinement,” Comput. Method. Appl. M., vol. 194, pp. 4135-4195, Oct. 2005.

[7] X. W. Gao, “A meshless BEM for isotropic heat conduction problems with heat generation and spatially varying conductivity,” Int. J. Numer. Meth. Eng., vol. 66, pp. 1411-1431, Dec. 2006.